Supplementary Information (SI) for Catalysis Science & Technology.

Construction of relay reaction system by Co@S-1 and In-Ce/H-Beta for selective catalytic reduction of nitrogen oxides with methane

Mingkang Zhang [1], Jinwei Wu [1], Junfei Chen [1], Haolin Yang [2,*], Xiaohan Wang [2], Zebao Rui [1,*]

[1] School of Chemical Engineering and Technology, Southern Marine Science and Engineering Guangdong Laboratory (Zhuhai), Guangdong Engineering Technology Research Center for Platform Chemicals from Marine Biomass and their Functionalization, Sun Yat-sen University, Zhuhai 519082, China

[2] CAS Key Laboratory of Renewable Energy, Guangdong Provincial Key Laboratory of New and Renewable Energy Research and Development, Guangzhou Institute of Energy Conversion, Chinese Academy of Sciences, Guangzhou 510640, China

** To whom correspondence should be addressed.*

E-mail address: ruizebao@mail.sysu.edu.cn (Zebao Rui); yanghl@ms.giec.ac.cn (Haolin Yang)

S1. Preparation of catalyst

Synthesis of InCo/H-Beta

The InCo/H-Beta/H-Beta sample was prepared by an ion exchange method. A certain amount of $InCl_3 \cdot 4H_2O$ and $Co(NO_3)_3$⑩$6H_2O$ were dispersed in a 100 mL deionized water solution with the In/Co mass ratio of 1:8. Then, 3 g of H-Beta molecular sieve was added, and the solution was stirred for 8 h at 85 °C. The product was washed and dried at 80 °C overnight. Finally, the sample was calcined at 500 °C for 3 h in air with a heating rate of 5 °C min $^{-1}$. The obtained catalyst was donated as InCo/H-Beta.

S2. Catalyst evaluation

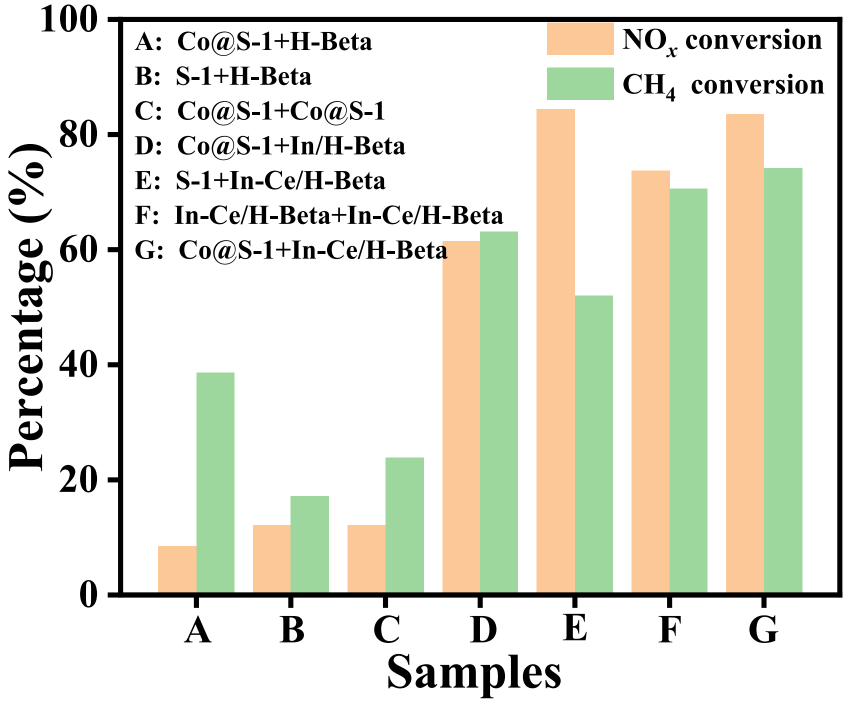

Fig. S1 CH_4-SCR performance comparison of various relay reaction systems at 500 °C. Reaction conditions: 500 ppm CH_4, 500 ppm NO, 5 vol.% O_2, balanced with Ar, $WHSV$= 60000 mL g^{-1} h^{-1}, $m_{cat.}$ = 0.2 g.

The catalyst activity for selective catalytic reduction of nitrogen oxides with methane (or CH_4-SCR) was evaluated on a fixed-bed reactor at 500 °C. Compared with S-1+In-Ce/H-Beta, the Co@S-1+In-Ce/H-Beta shows a much higher CH_4 conversion activity. This activity improvement is attributed to the redox properties of CoO_x sites on the Co@S-1.[1,2] Notably, the Co@S-1+H-Beta shows a lower NO_x conversion activity than Co@S-1+In-Ce/H-Beta, suggesting that In-Ce/H-Beta holds high NO_x conversion activity because of the exit of InO^+ active sites.[3]

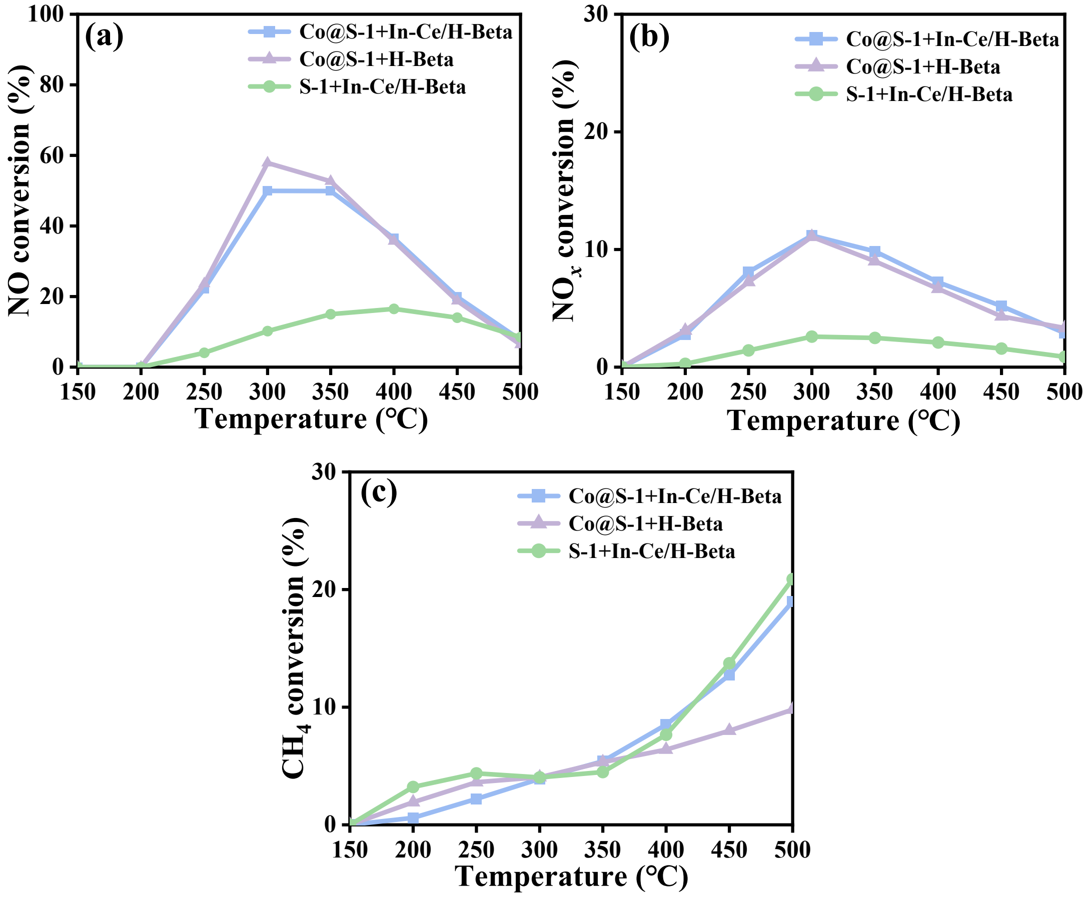

Fig. S2 Performance comparison of various relay reaction systems at different gas compositions: (a & b) 500 ppm NO+ 5 vol.% O_2, (c) 500 ppm CH_4+5 vol.% O_2; balanced with Ar, *WHSV*= 60000 mL g^{-1} h^{-1}, $m_{cat.}$=0.2 g.

To identify the role of Co@S-1 and In-Ce/H-Beta in CH_4-SCR reaction, the catalytic activity of various relay reaction systems (or RRS), i.e., Co@S-1+In-Ce/H-Beta, Co@S-1+H-Beta, and S-1+In-Ce/H-Beta were evaluated under various gas compositions. As illustrated in Fig. S2a, the Co@S-1+H-Beta RRS exhibits superior NO conversion capability compared to other catalysts under NO+O_2 gaseous composition. Additionally, S-1+In-Ce/H-Beta RRS exhibits the lowest NO_x conversion compared to other RRS (Fig. S2b), due to the absence of Co@S-1 catalyst for NO oxidation. Under the atmosphere of CH_4 + O_2 (Fig. S2c), the CH_4 conversion rates are ordered as Co@S-1+In-Ce/H-Beta ~ S-1+In-Ce/H-Beta > Co@S-1+H-Beta, suggesting that the In-Ce/H-Beta possesses favorable activity of CH_4 conversion.

As observed in Fig. S3a, the NO oxidation performance of the Co@S-1+In-Ce/H-Beta relay reaction system exhibits an initial enhancement followed by a subsequent decline with increasing mass ratio of Co@S-1 in the relay reaction system. Furthermore, Fig. S3b&c demonstrates that the CH_4-SCR performance progressively improves with elevated mass ratios of In-Ce/H-Beta in the relay reaction system. However, the enhancement became less pronounced when the In-Ce/H-Beta loading is increased from 0.1 g to 0.15 g. Notably, an optimal mass ratio is identified, where the relay reaction system achieves maximum CH_4-SCR efficiency when the Co@S-1 and In-Ce/H-Beta maintain a mass ratio of unit.

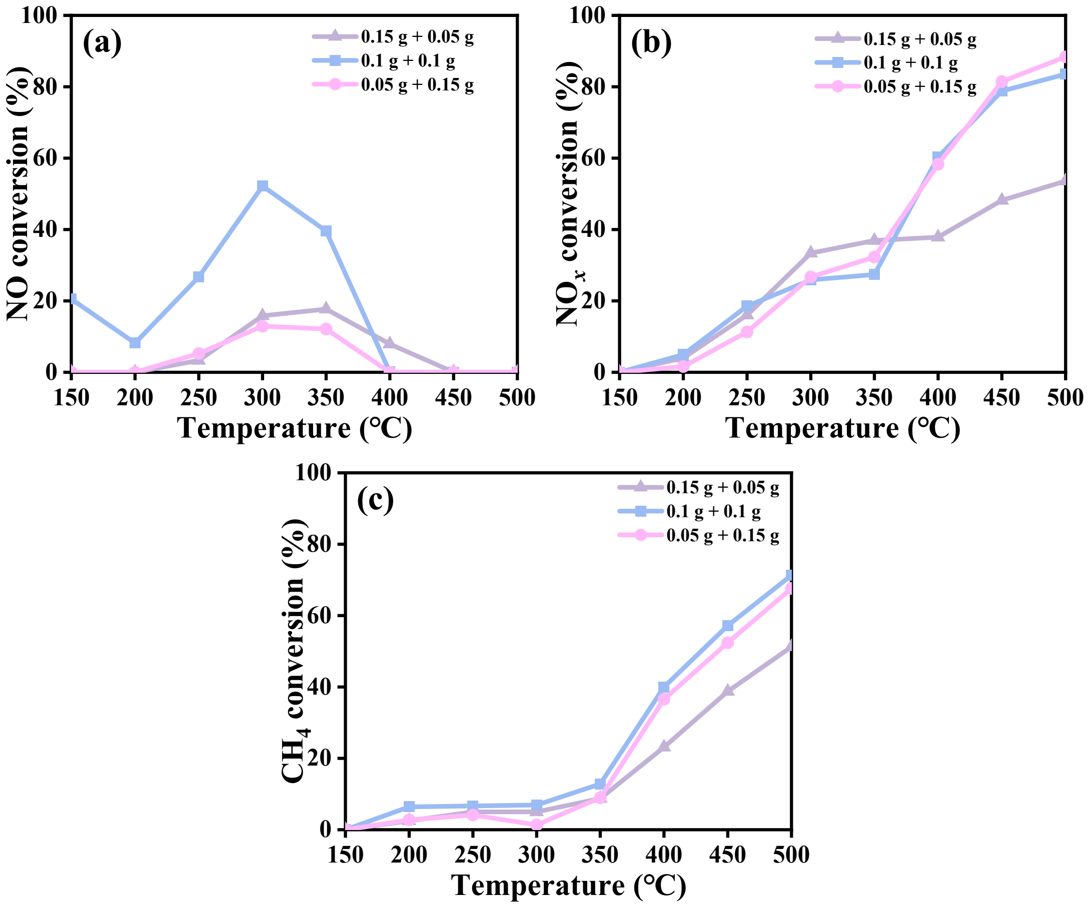

Fig. S3 Effect of relay catalysts mass ratio on (a) NO, (b) NO$_x$, and (c) CH$_4$ conversions over Co@S-1 + In-Ce/H-Beta relay reaction system. Reaction conditions: 500 ppm CH$_4$, 500 ppm NO, 5 vol.% O$_2$, balanced with Ar, $WHSV$= 60000 mL g^{-1} h^{-1}, $m_{\text{cat.}}$ = 0.2 g.

To investigate the effectiveness of direct cobalt incorporation into In/H-Beta catalysts for CH$_4$-SCR performance, catalytic evaluations were conducted on three distinct systems: S-1+InCo/H-Beta, Co@S-1+H-Beta, and Co@S-1+In/H-Beta. As illustrated in Fig. S4, comparative analysis reveals that the S-1+InCo/H-Beta exhibits inferior CH$_4$-SCR activity compared to the other two catalysts. This observation demonstrates that cobalt doping into In/H-Beta zeolite systems fails to enhance catalytic performance for CH$_4$-SCR applications.

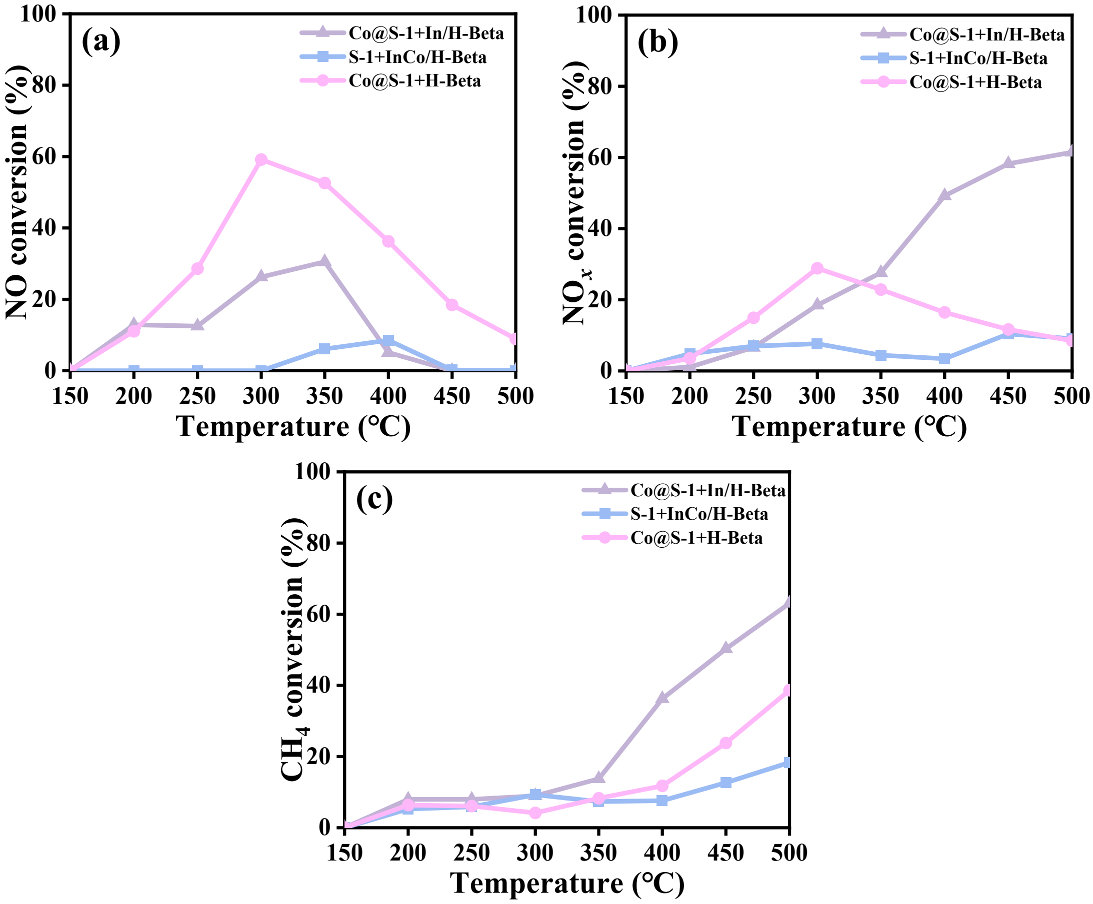

Fig. S4 (a) NO, (b) NO_x, and (c) CH_4 conversion over various relay reaction systems. Reaction conditions: 500 ppm CH_4, 500 ppm NO, 5 vol.% O_2, balanced with Ar, *WHSV*= 60000 mL g^{-1} h^{-1}, $m_{cat.}$ = 0.2 g.

As compared in Fig. S5, the sequential loading of the catalysts (Co@S-1+In-Ce/H-Beta) leads to remarkably better CH_4-SCR performance than the physical mixture of Co@S-1&In-Ce/H-Beta. Although the NO_x conversions of Co@S-1+Co@S-1are highest among the samples at temperatures lower than 350 ^{o}C, its NO_x conversion decreases rapidly and is greatly lower than those of Co@S-1+In-Ce/H-Beta with further increasing reaction temperatures (Fig. S5b). In spite of the high CH_4 activation ability of In-Ce/H-Beta, the CH_4 conversions of Co@S-1+In-Ce/H-Beta are comparable with those of In-Ce/H-Beta+In-Ce/H-Beta (Fig. S5c). As evidenced in Fig. S5d, a progressive decline in CH_4 selectivity is observed for both Co@S-1+In-Ce/H-Beta and Co@S-1&In-Ce/H-Beta systems as the temperature increases beyond 400 °C, indicating the gradual predominance of CH_4 oxidation over the selective catalytic reduction of nitrogen oxides by CH_4. Notably, the relay catalytic system (Co@S-1+In-Ce/H-Beta) demonstrates superior CH_4 selectivity performance compared to the physically mixed system (Co@S-1&In-Ce/H-Beta). This comparative analysis underscores the enhanced efficacy of the relay catalytic system in optimizing CH_4-SCR. These results indicate the sequential relay catalysis character of Co@S-1+In-Ce/H-Beta and its promotion to CH_4-SCR.

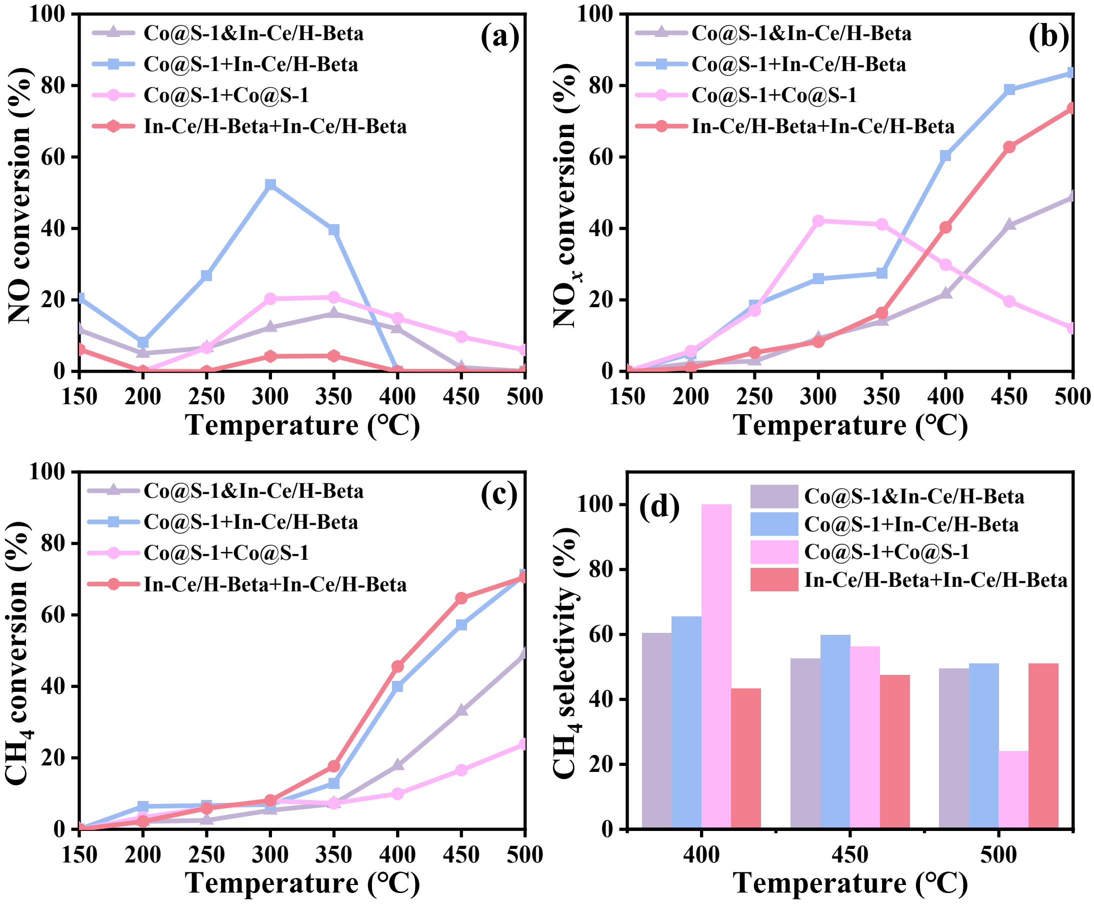

Fig. S5 CH_4-SCR performance comparison of various relay reaction systems. Reaction conditions: 500 ppm CH_4, 500 ppm NO, 5 vol.% O_2, balanced with Ar, *WHSV*= 60000 mL g^{-1} h^{-1}, $m_{cat.}$ = 0.2 g.

Table S1. Experimental details and performance comparison of Co@S-1+In-Ce/Beta with typical reported catalysts in the literature for CH_4-SCR

Samples	Gas composition	*WHSV* (mL h^{-1} g^{-1})	*T* (°C)	NO$_x$ conversion(%)	CH_4 conversion (%)	Ref.
Co@S-1+In-Ce/Beta	500 ppm CH_4+500 ppm NO +5% O_2+Ar	60000	250	18	7	This work
			350	27	13	
			450	79	57	
In-Beta81	500 ppm CH_4+500 ppm NO+ 2% O_2+Ar	23600	450	50	52	4
$Co_{3.0}$-$Pd_{0.15}$-SiBEA	150 ppm NO+1500 ppm CH_4+7% O_2+He	40000	250	40	0	5
			350	48	5	
			450	52	25	
Ce/HZSM-5-CoOx	1000 ppm CH_4+1000 ppm NO+2% O_2+N_2	15000	350	26	12	6
Pd-In-HMOR	4000 ppm NO+4000 ppm CH_4+2% O_2	15000	350	25	10	7
			450	42	30	
Co-SSZ-13	1000 ppm NO+1000 ppm CH_4+4% O_2+N_2	10000	450	72	51	8
Co, Ag-ZSM-5	1000 ppm NO+5000 ppm CH_4+2% O_2+He	6000	350	95	8	9
			450	95	45	
In-Co_3O_4/H-Beta	400 ppm NO+400 ppm CH_4+100 ppm SO_2+10% O_2+5% H_2O+Ar	23600	550	40	38	10

S3. Morphology and structure

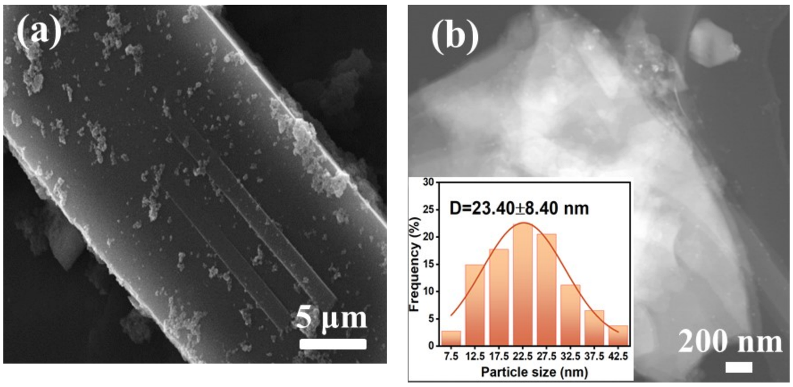

Fig. S6 (a) SEM image and (b) STEM image and metal particle size distribution of Co@S-1

SEM and STEM images of Co@S-1 are presented in Fig. S4. The Co@S-1 catalyst TEM characterization in Fig. S4b indicates that the nanoparticle structure with a size of ca. 23 nm.

Table S2 Texture properties and composition information of the employed samples.

Catalysts	S_{BET} ($m^2 \cdot g^{-1}$) [a]	V_{total} ($cm^3 \cdot g^{-1}$) [a]	V_{micro} ($cm^3 \cdot g^{-1}$) [a]	V_{meso} ($cm^3 \cdot g^{-1}$) [a]	In loading (wt.%) [b]	Ce loading (wt.%) [b]	Co loading (wt.%) [b]
In-Ce/H-Beta	521.2	0.539	0.164	0.375	2.05	0.5	-
Co@S-1	362.6	0.667	0.096	0.571	-	-	12.12

[a] calculated by BET formula

[b] measured by ICP-AES

S4. Chemical properties

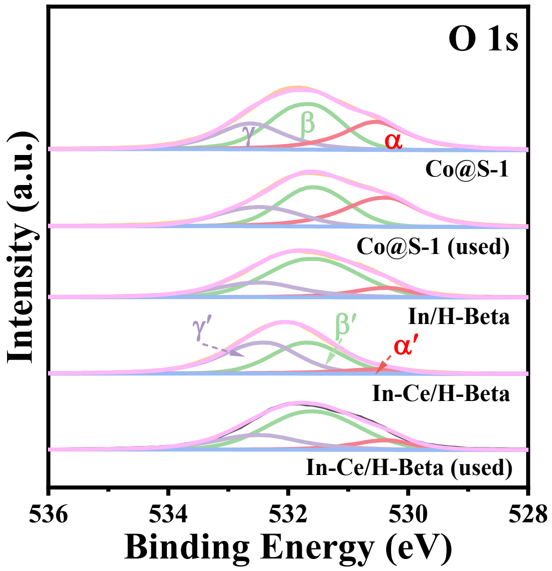

Fig. S7 O 1s XPS spectra of catalysts

As shown in Fig. S7, the O_α, O_β, and O_γ peaks in the O 1s spectrum of Co@S-1 can be attributed to the lattice oxygen of Co_3O_4 crystallites, surface-adsorbed oxygen, and the Si-O-Si or Si-O-Co species, respectively.[11,12] Wherein, the surface-adsorbed oxygen species are reported to play a pivotal role in modifying reaction energy and activating reactants, thereby facilitating NO_x reduction.[13] The $O_{\alpha'}$, $O_{\beta'}$, and $O_{\gamma'}$ peaks in the O 1s spectrum of In-Ce/H-Beta can be attributed to the indium oxide, lattice oxygen in HBEA zeolite, and surface oxygen species, respectively.[14,15] The surface oxygen species possesses high mobility and can actively participate in the oxidation process.[16] After the long-time stability test, the relative amounts of O_α, O_β, and O_γ peaks in the Co@S-1 (used) and the relative amounts of $O_{\alpha'}$, $O_{\beta'}$, $O_{\gamma'}$ in the In-Ce/H-Beta (used) all show an obvious change, as compared in Table S3.

Table S3 XPS-derived chemical compositions of the samples

Catalysts	Co species (%)		Co^{3+}/Co^{2+}	Ce species (%)		Ce^{3+}/Ce^{4+}	In species (%)		O species (%)		
	Co^{3+}	Co^{2+}		Ce^{3+}	Ce^{4+}		In_2O_3	InO^+	O_α	O_β	O_γ
Co@S-1	31.5	68.5	0.46	-	-		-		29.9	44.3	25.8
Co@S-1 (used)	21.9	78.1	0.28	-	-		-		35.9	40.3	23.8
In/H-Beta	-	-		-	-		45.9	54.1	9.2	43.2	47.6
In-Ce/H-Beta	-	-		43.6	56.4	0.77	38.5	61.5	7.0	43.3	49.7
In-Ce/H-Beta (used)	-	-		45.9	54.1	0.85	38.9	61.1	11.5	63.7	24.8

Table S4 Calculated NH_3 desorption amount of catalysts from NH_3-TPD profiles

Sample	NH_3 desorption of different peaks (mmol g^{-1}) [a]				Total NH_3 desorption (mmol g^{-1}) [a]
	α	β	θ	γ	
In-Ce/H-Beta	0.376	0.469	0.464	1.309	2.619
Co@S-1	0.338	0.321	0.333	0.264	1.257

[a] The NH_3 desorption of each peak was calculated according to the standard curve of NH_3 amount versus peak area.

S5. *In-situ* DRIFTS study

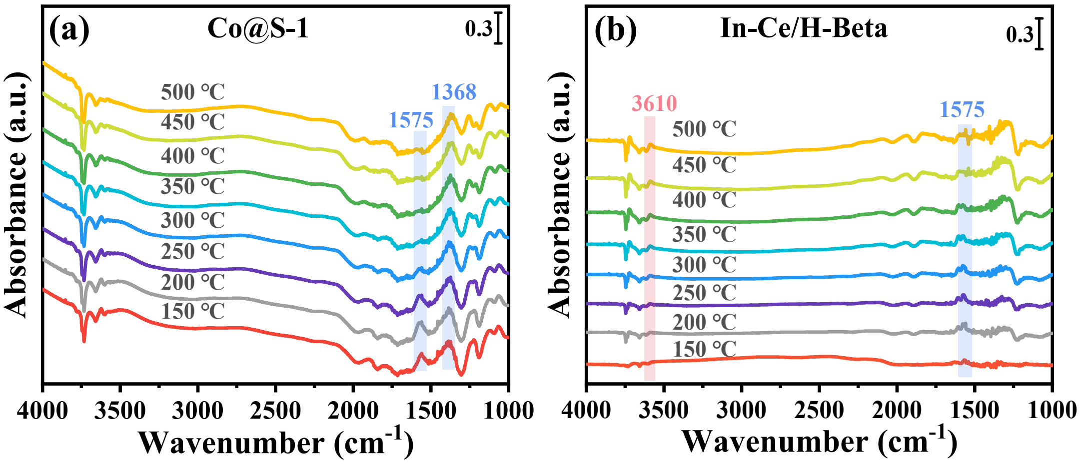

Fig. S8 *In-situ* DRIFTS spectra of NO + O_2 + Ar gas mixture adsorption over (a) Co@S-1 and (b) In-Ce/H-Beta versus temperatures. Reactant gas: 500 ppm NO +5 vol.% O_2, balanced with Ar, *WHSV*=60000 mL g^{-1} h^{-1}.

Fig. S8 shows *in-situ* DRIFTS spectra of Co@S-1 and In-Ce/H-Beta with an exposure to NO + O_2+Ar. As depicted in Fig. S8a, the intensity of bands at 1575 cm^{-1}(NO-3 species) decreases with the increase in temperature,[17] indicating that the NO-3 species is formed over Co@S-1 below 300 °C. Furthermore, the intensity of the ionic nitrates band at 1368 cm^{-1} remains consistent with the increase in temperature, indicating that ionic nitrates on the Co@S-1 catalyst possess well thermal stability.[18] The absorption peak at 3610 cm^{-1} is observed on In-Ce/H-Beta (Fig. S8b), which is assigned to the stretching vibration of the bridging hydroxyl group ($H^{+}Z^{-}$) on the Brønsted acid of the zeolite.[19,20] The intensity enhancement of the $H^{+}Z^{-}$ band of the acidic hydroxyl groups is partly due to the replacement of the protons by NO^{+} .[21] Notably, the NO-3 species absorption band at 1575 cm^{-1} is consistently detected on In-Ce/H-Beta from 150 °C to 500 °C, suggesting the In-Ce/H-Beta can produce NO-3 species with enhanced thermal stability.

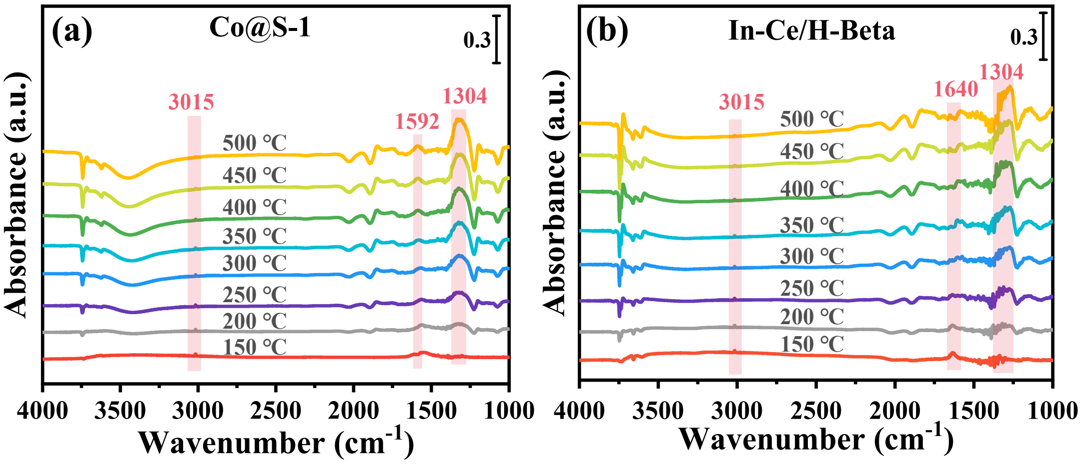

Fig. S9 *In-situ* DRIFTS spectra of CH_4 + O_2 + Ar gas mixture adsorption over (a) Co@S-1 and (b) In-Ce/H-Beta versus temperatures. Reactant gas: 500 ppm CH_4+5vol.% O_2, balanced with Ar, *WHSV*=60000 mL g^{-1} h^{-1}.

Fig. S9 shows *in-situ* DRIFTS spectra of Co@S-1 and In-Ce/H-Beta with an exposure to CH_4 + O_2 + Ar. The bands observed at 3014 cm^{-1} and 1303 cm^{-1} over two catalysts correspond to the stretching vibration of the C-H bond of the adsorbed gaseous

CH_4,[22] indicating that the ability of two catalysts to adsorb and activate CH_4. The peak at 1592 cm^{-1} is associated with the carbonate species (CO_3*),[23] and the intensity of carbonate species increases with the increase in temperature.

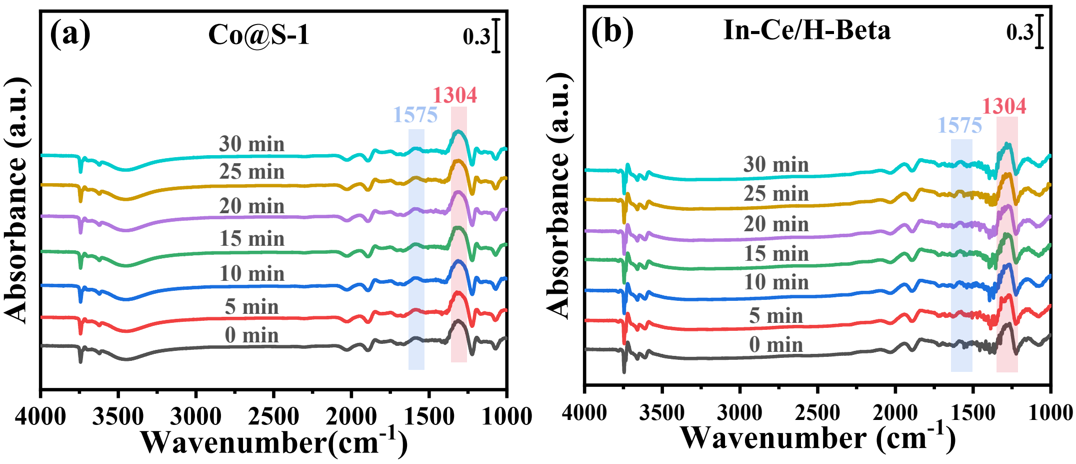

Fig. S10 *In-situ* DRIFTS spectra of CH_4 + NO + O_2 + Ar gas mixture adsorption over (a) Co@S-1 and (b) In-Ce/H-Beta versus times at 500 ^{o}C. Reactant gas: 500 ppm CH_4 + 500 ppm NO + 5vol.% O_2**,** balanced with Ar, *WHSV*=60000 mL g^{-1} h^{-1}.

Fig. S10 shows *in-situ* DRIFTS spectra of Co@S-1 and In-Ce/H-Beta with an exposure to CH_4 + NO + O_2 + Ar at 500 °C. After a 30-minute exposure to the CH_4 + NO + O_2 atmosphere, the peak intensities at 1575 cm^{-1} (NO-3) and 1304 cm^{-1} (C-H bond) on both catalysts remain constant,[17,22] suggesting that both catalysts exhibit excellent thermal stability in the activation of CH_4 and the generation of NO-3 at this temperature.

Reference

1 X. Fan, L. Li, F. Jing, J. Li and W. Chu, *Fuel*, 2018, 225, 588–595.

2 X. Xie, Y. Li, Z.-Q. Liu, M. Haruta and W. Shen, *Nature*, 2009, 458, 746–749.

3 H. Schwarz, *Angew. Chem. Int. Ed.*, 2011, 50, 10096–10115.

4 J. Zhao, G. Zhang, J. He, Z. Wen, Z. Li, T. Gu, R. Ding, Y. Zhu and R. Zhu, *Chemosphere*, 2020, 252, 126458.

5 A. Rodrigues, P. Da Costa, C. Méthivier and S. Dzwigaj, *Catal. Today*, 2011, 176, 72–76.

6 F. Huang, W. Hu, J. Chen, Y. Wu, P. Qu, S. Yuan, L. Zhong and Y. Chen, *Ind. Eng. Chem. Res.*, 2018, 57, 13312–13317.

7 H. Decolatti, H. Solt, F. Lónyi, J. Valyon, E. Miró and L. Gutierrez, *Catal. Today*, 2011, 172, 124–131.

8 S. Han, X. Tang, Y. Ma, Q. Wu, J. Shi, J. Li, X. Meng, A. Zheng and F.-S. Xiao, *J. Phys. Chem. C*, 2021, 125, 16343–16349.

9 X. Chen, A. Zhu, C. T. Au and C. Shi, *Catal. Lett.*, 2011, 141, 207–212.

10 J. Zhao, Z. Wen, R. Zhu, Z. Li, R. Ding, Y. Zhu, T. Gu, R. Yang and Z. Zhu, *Chem. Eng. J. Adv.*, 2020, 3, 100029.

11 S. Song, J. Li, Z. Wu, P. Zhang, Y. Sun, W. Song, Z. Li and J. Liu, *AIChE J.*, 2022, 68, e17451.

12 L. Zhang, S. Huang, W. Deng, D. Yang, Q. Tang, S. Zhu, and L. Guo, *Microporous Mesoporous Mater.*, 2021, 312, 110599.

13 J. S. Yoo, T. S. Khan, F. Abild-Pedersen, J. K. Nørskov and F. Studt, *Chem. Commun.*, 2015, 51, 2621–2624.

14 Y. Shi, X. Wang, L. Chen, S. Li, C. Wu, S. Shan and W. Li, *Appl. Surf. Sci.*, 2020, 506, 144715.

15 L. B. Hoch, T. E. Wood, P. G. O’Brien, K. Liao, L. M. Reyes, C. A. Mims and G. A. Ozin, *Adv. Sci.*, 2014, 1, 1400013.

16 T. Gu, Y. Liu, X. Weng, H. Wang and Z. Wu, *Catal. Commun.*, 2010, 12, 310–

313.

17 R. Q. Long and R. T. Yang, *J. Catal.*, 2000, 194, 80–90.

18 C. Zhang, G. Xu, Y. Zhang, C. Chang, M. Jiang, L. Ruan, M. Xiao, Z. Yan, Y. Yu and H. He, *Appl. Catal. B Environ. Energy*, 2024, 348, 123820.

19 M. Iwasaki and H. Shinjoh, *J. Catal.*, 2010, 273, 29–38.

20 M. Rivallan, G. Ricchiardi, S. Bordiga and A. Zecchina, *J. Catal.*, 2009, 264, 104–116.

21 J. Xu, Y. Zhang, X. Xu, X. Fang, R. Xi, Y. Liu, R. Zheng and X. Wang, *ACS Catal.*, 2019, 9, 4030–4045.

22 L. Jiang, D. Li, G. Deng, C. Lu, L. Huang, Z. Li, H. Xu, X. Zhu, H. Wang and K. Li, *Chem. Eng. J.*, 2023, 456, 141054.

23 K. Li, K. Liu, D. Xu, H. Ni, F. Shen, T. Chen, B. Guan, R. Zhan, Z. Huang and H. Lin, *Chem. Eng. J.*, 2019, 369, 660–671.